

**Junying Wang**  
 Turbomachinery Laboratory,  
 State Key Laboratory of Automotive  
 Safety and Energy,  
 Tsinghua University,  
 Beijing 100084, China

**Xinqian Zheng<sup>1</sup>**  
 Turbomachinery Laboratory,  
 State Key Laboratory of Automotive  
 Safety and Energy,  
 Tsinghua University,  
 Beijing 100084, China;  
 Department of Aerodynamics and  
 Thermodynamics,  
 Institute for Aero Engine,  
 Tsinghua University,  
 Beijing 100084, China  
 e-mail: zhengxq@tsinghua.edu.cn

# Review of Geometric Uncertainty Quantification in Gas Turbines

*Due to the manufacturing error and in-service degradation of gas turbines, there is always a deviation between the actual geometry and the design geometry. This geometric deviation has a prominent uncertainty characteristic, resulting in a dispersion of the gas turbine performance and thereby reducing the manufacturing qualification rate and service life. As the performance and reliability requirements of gas turbines increase continually, more and more attention has been paid to the quantitative study of the effect of the geometric uncertainty on performance. In this paper, the main sources and features of gas turbine geometric uncertainty are reviewed first. Then, the basic principles, characteristics, and application in gas turbines of different uncertainty quantification (UQ) methods are reviewed. Finally, the progress, challenges, and prospects for correlational research are summarized in the conclusion. [DOI: 10.1115/1.4047179]*

**Keywords:** uncertainty quantification, gas turbine, fan, compressor, turbine

## 1 Introduction

**1.1 Background.** Gas turbines are widely used in aviation, power stations, military applications, and other fields. As the core components in gas turbines energy conversion process, turbomachinery components such as the fan, compressor, and turbine are directly related to the performance and service life of the entire device.

However, due to the manufacturing error and in-service degradation, there are various unavoidable geometric deviations from the design geometry in the fan, compressor, and turbine. During the manufacturing process, factors that may cause the geometric deviation include the inherent geometric errors of the processing system, mechanical deformation/thermal deformation of the processing system, internal strains of the workpiece, and assembly errors of the workpiece. On the other hand, during the operation process, factors such as corrosion, erosion, oxidation, and fouling will lead to geometric deviations. This geometric deviation has a prominent uncertainty characteristic, resulting in a dispersion of the gas turbine performance and thereby reducing the manufacturing qualification rate and service life. In recent years, with the increase of the performance and reliability requirements of gas turbines, the sensitivity of performance to the geometric uncertainty increase continually and the requirement for geometric accuracy is rising gradually. Therefore, more and more attention has been paid to the quantitative study of the effect of the geometric uncertainty on performance.

Through the quantitative study of uncertainty, the distribution characteristics of the gas turbine performance can be obtained, and the performance qualification rate can be evaluated [1,2]. Moreover, the key geometric parameters with important impacts on performance can be identified and the corresponding tolerances can be optimized, which can lay the foundation for the improvement to the design, manufacturing, and maintenance processes [1,3]. Also, geometric robustness design optimization based on the quantitative results can help improve the gas turbine performance and life and reduce the overall cost [2].

**1.2 Uncertainty Quantification Methods.** The deterministic simulation method cannot take into consideration the influence of uncertainty factors [4]. Therefore, uncertainty quantification (UQ)

methods have been developed rapidly as an effective way to deal with various uncertainty problems [5]. A series of UQ methods have been applied to the research of gas turbines, among which the sampling-based method is the simplest in principle and direct to implement through random simulation [6]. However, the sampling-based method requires a large number of simulation calculations. In this instance, surrogate-model-based methods and polynomial chaos (PC) methods [7] have been developed as low-cost alternatives to the original high-fidelity simulation model to predict gas turbine performance. Also, the performance and geometric variables are approximately linearly dependent under a small variation range [8]. Under this assumption, the sensitivity-based method can be adopted to greatly save computing resources [9].

**1.3 Review Aims.** In recent years, significant research progress has been made in UQ methods applied to gas turbines. Several methods with different advantages/disadvantages have been developed to deal with UQ problems in different situations. However, there are still some challenges in this field. The purpose of this paper is to summarize predominant geometric uncertainty variables due to out-of-tolerance manufacturing and in-service deterioration, and to review the state-of-the-art research progress and challenges and to propose research prospects of UQ studies in the gas turbine field. The objects of this review are focused on the fan, compressor, and turbine. In the following part of this paper, the main sources and features of gas turbine geometric uncertainty are reviewed first. Then, the basic principles, characteristics, and application in gas turbines of different uncertainty quantification methods are reviewed, including sampling-based method, sensitivity-based method, surrogate model-based method, and PC method. Finally, the progress, challenges, and prospects for correlational research are summarized in the conclusion and recommendation sections.

## 2 Sources of Geometric Uncertainty in Gas Turbine

Geometric uncertainties in gas turbines mainly occur during the manufacturing and in-service processes. As shown in Fig. 1, almost every component of a gas turbine will be influenced by geometric uncertainties. Moreover, the main characteristics and effects of geometric uncertainties from different sources are different. The purpose of this section is to give a review of observations and documented cases about geometric uncertainties from

<sup>1</sup>Corresponding author.

Manuscript received August 20, 2019; final manuscript received April 4, 2020; published online June 30, 2020. Assoc. Editor: Phillip Ligani.

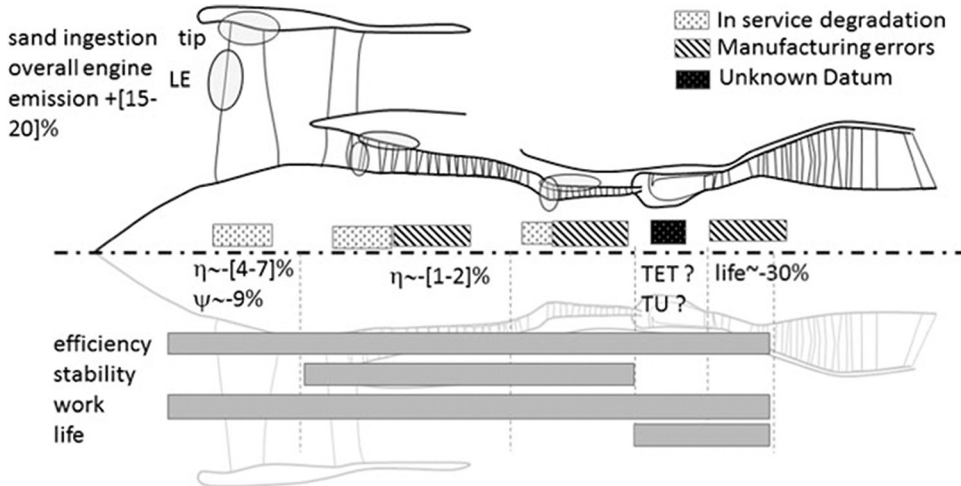


Fig. 1 Uncertainty due to in-service degradation and manufacturing errors in a turbofan [4]

both sources, identify the associated influencing factors, and summarize effects on performance.

**2.1 Manufacturing Geometric Uncertainty.** Due to different geometric and aerodynamic characteristics of the fan, compressor, and turbine, the effects of geometric uncertainties are diverse in different components. Therefore, the geometric uncertainties are reviewed separately for different parts.

**2.1.1 Fan.** A fan is usually used in the turbofan engine as the first compression component, and it is characterized by the large volume, high flowrate, and low-pressure ratio [10]. A typical manufacturing process of a fan blade can be found from Ref. [11].

The blade surface geometric data can be obtained by optical scanning of a manufactured fan blade, based on which the geometric uncertainty model can be constructed. In this process, an effective method is principal component analysis (PCA), which is a widely used statistical dimensionality reduction technique. The principle is to find a few uncorrelated principal components (eigenmodes) to retain as much information as possible of the original variables. Detailed mathematical derivation and application methods are described in Refs. [2] and [12]. A typical PCA study on the fan is executed by Schnell et al. [1], based on geometric measured data of nine rotor blades of a counter-rotating turbofan. The PCA results indicate that the first four eigenmodes can already contain 99.1% of the cumulated geometric uncertainty (shown in Fig. 2). In addition, the correspondences between each eigenmode and dimensionless design parameters can be found in Ref. [1], which indicates visible uncertainty of the leading-edge bluntness, leading-edge radius, chord, and leading-edge metal angle. Based on the PCA results, a geometric uncertainty model can be constructed and then used for UQ analysis (as shown in Sec. 4).

Also, to assess the overall influence, full-stage three-dimensional (3D) computational fluid dynamics (CFD) simulations are conducted for each of the nine blades at 100% speed. The results indicate that the fluctuation interval of isentropic efficiency is within  $\Delta\eta_{is} = \pm 0.05\%$  at most of the operating conditions while the fluctuation at the near instability point increases to  $\pm 0.1\%$ . Therefore, it is indicated that a given geometric deviation can produce different degrees of influence on performance in different working conditions. Moreover, the standard deviation of the total pressure ratio is about  $\Delta\pi_t = 0.0008$  at almost all operating points [1]. This indicates that the impact of fan blade manufacturing error on the performance can be relatively small under a high manufacturing accuracy.

The implementation of PCA requires sufficient measured blade geometric data. However, in many studies related to gas turbines, high-resolution measurement data for new or used blades is not

available. In the absence of such data, heuristic information such as expert opinions and experience can be adopted to describe geometric uncertainty. Also, known statistical features can be used to construct geometric uncertainty models of similar blades (e.g., blades manufactured by the same process) [2].

For manufacturing geometric uncertainty of fans, researches based on heuristic information mainly focused on blade leading edge, as the leading edge is considered to be the most influential geometric factor in the transonic flow field in fans [1]. A thinner leading-edge profile can reduce the shock loss near the leading edge, especially in supersonic flow, which in turn reduces overall losses [8]. By optimizing the leading edge, Giebmanns et al. [8] increase the total pressure ratio and isentropic efficiency of a fan, with the highest efficiency increasing by 0.5% relatively.

In addition, the seal leakage flow at the rear of a fan can also impact performance. The experimental result from Zamboni et al. [13] shows that the secondary flow in the core blade channel interacts with fan seal leakage flow, bringing about high losses in the hub area. For a fan with a bypass ratio of 7.7 and a stator behind it, when there is a 1.5% leakage flowrate, the loss increases to three times that of 0% leakage flow, and the flow capacity is reduced by 6.5%.

In summary, the impact of manufacturing geometric uncertainty on fan performance can be relatively small under a high manufacturing accuracy. However, shorter fan axial distances and more sensitive design of core engine also continue to enhance the effects of manufacturing geometric uncertainty on fan performance [4].

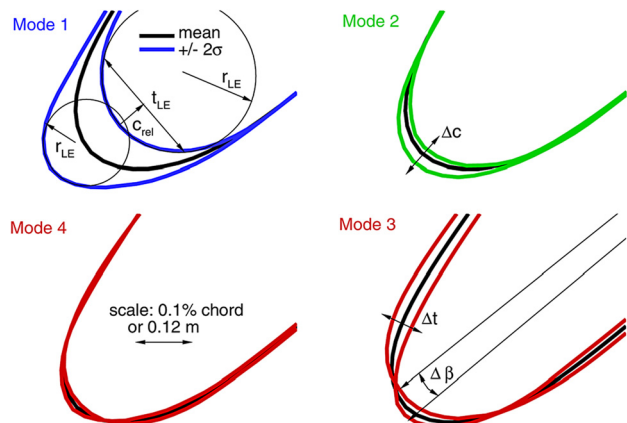


Fig. 2 Shapes of the first 4 modes from PCA and defined non-dimensional parameters to characterize each mode [1]

**2.1.2 Compressor.** Different from the fan, the size of a compressor is usually small, and thus, the relative geometric uncertainty is larger under the same manufacturing precision, bringing about a more considerable influence on the performance [4]. Moreover, a strong adverse pressure gradient further enlarges the effect of geometric uncertainty. Therefore, the influence of the geometric uncertainty on compressor performance has attracted much attention. In addition, for aviation applications, as the requirements for light-weighting increase, the size of the compressor is continuously reduced, leading to higher requirements on geometric accuracy.

The compressor geometric uncertainty model can be constructed by the PCA method [2], which is originally introduced by Garzon [2] based on the surface measurement results of 150 compressor rotor blades. PCA results indicate that the first six eigenmodes can contain 99% of the total scatter in the original measurement data, and there is non-negligible maximum thickness uncertainty, trailing edge angle uncertainty, leading-edge radius uncertainty while there is no significant uncertainty of chord length in the measured airfoils. The advantage of PCA is that it can be used to analyze and describe any type of geometric uncertainty. However, the principal components extracted do not directly correspond one to one with the design parameters which are more familiar to engineers. Therefore, Lange et al. [14] proposed a new probabilistic model for compressor blades, which can convert measured blade profile into uncertainty features of typical blade profile parameters, such as chord length, stagger angle, leading-edge thickness, and trailing edge thickness.

In addition to the researches based on geometric measurement data, many studies directly focus on some critical geometric parameters to explore the impact on compressor performance. Marson [15] summarizes possible manufacturing uncertainties of compressor blades, among which several parameters have attracted much attention in existing researches, including leading-edge shape, tip clearance, surface roughness, and some other parameters, as described below.

**Blade leading edge.** The compressor blade leading edge has an important effect on performance. In addition, due to the small value of leading-edge radius, which can be only 0.2–0.5 mm in a typical transonic or supersonic compressor [16,17], leading-edge uncertainty may be very serious due to insufficient machining accuracy, blade surface coating, or other processing errors. For example, a typical blade surface uniform coating with a thickness of 0.025 mm [16] can increase the leading-edge radius by over 10%.

Studies have shown that the leading-edge shape change will reduce aerodynamic efficiency mainly by increasing shock losses [18], flow separation losses [19,20], or the wake/leading-edge interaction [17]. It is also worth reminding that the influence will be different under different conditions. For example, the relative total pressure loss of a transonic compressor rotor increases more quickly with the leading-edge radius under a higher Mach number [18]. In addition, experimental research on the transonic Rotor 14 also shows that the influences are more visible at higher speed: when the leading-edge thickness near the blade tip is doubled, the highest efficiency reduced by 3.5% at design speed while no apparent performance deterioration appears at lower speeds (90% and 70% design speed) [20]. By quantifying the effect of the leading-edge shape on the performance, the precision control of each manufacturing process can be guided such as the coating process [16]. Also, the leading-edge uncertainty will change the compressor operating range [21]. According to the experience from isolated airfoils, the blunt and smooth leading edge can provide a wider working range. Herring et al. [22] obtain results consistent with the isolated airfoil experience under lower speed and higher pitch conditions. However, Carter's experimental results under typical Mach number and pitch conditions indicate that a smaller leading-edge radius will result in a wider operating range, especially at high speeds [19].

In addition, it is worth noting that although the leading-edge shape is important to compressor performance, the manufacturing

tolerance is difficult to be measured: the error of optical measurement is usually about 15  $\mu\text{m}$  and can reach more than 10% of the leading-edge thickness [4].

**Blade tip clearance.** Blade tip clearance is another important parameter [23] which has a great influence on compressor efficiency, especially in the high pressure (HP) stages. Factors affecting the tip clearance during manufacturing and assembly mainly include: component thermal expansion; deformation under a load of components; dimensional tolerance and position in the manufacturing process; buckling caused by uneven heating and loading; component position changes caused by the fit clearance [24].

The increase in tip clearance can reduce compressor pressurization capacity and efficiency. Based on a large number of experimental data [25], it has been summarized that when the rotor tip clearance is larger than 1% of the chord length, there is almost a linear relationship: 1% of chord length increase in tip clearance will lead to 4.6% losses of the peak pressure rises. As for efficiency, research based on a single-stage axial compressor [26] showed that when the rotor tip clearance is less than 0.8% span, there is an optimum clearance to maximize efficiency. When the rotor tip clearance is between 0.8% and 3.4% span, the relationship between tip clearance and efficiency is almost linear, and when tip clearance increases by 1% span, efficiency decreases about 1%, which is mainly caused by the leakage flow mixing. Finally, when the tip clearance is greater than 3.4% span, the sensitivity of efficiency to tip clearance is reduced due to a weakened mixing loss. Moreover, for multistage axial compressors, the tip clearance uncertainty will also change the matching between different stages. As tip clearance increases, the front stage operating point tends to be closer to the surge point while that of the rear stage tends to be closer to the choke point, thus causing a worsened matching resulting in higher efficiency losses [27].

Moreover, tip clearance also affects compressor operational stability. Vo [28] points out that there is a close relationship between blade tip region flow and the rotating stall phenomenon that occurs when the compressor internal flow is unstable. Baghdadi [29] has collected a large amount of experimental data which indicates that when the tip clearance is less than 1% of the chord length, compressor stability is not sensitive to tip clearance. However, within the conventional tip clearance range (1.5–3% chord length), the tip clearance and compressor surge margin are almost linear, and when tip clearance increases by 1% chord length, surge margin is reduced by about 8% relative to the maximum surge margin.

**Blade surface roughness.** Blade surface roughness resulting from the manufacturing process is also a significant parameter in the compressor [30]. When the blade surface is rough, the blade friction loss will increase, while when the surface roughness is reduced to a certain extent, it will not affect compressor performance, which is considered to be aerodynamically smooth. Research on a single-stage axial compressor [31] shows that compared with the rough machined blade, both hand-filed and highly polished blades can improve efficiency significantly while there is almost no difference between hand-filed and highly polished blades.

In addition, the effect of roughness varies with position and condition. Experimental analysis [32] showed that the surface roughness near the leading-edge and peak-suction regions is very influential to performance, especially in the design condition or conditions with less mass flowrate. According to measurements by Bons [30], the loss difference between rough and smooth blades of a HP compressor cascade will increase with  $\text{Re}_c$  when  $\text{Re}_c$  is in the range of  $3 \times 10^5$  to  $1 \times 10^6$ . Moreover, as the density and hence  $\text{Re}_c$  in the HP compressor is much higher than that in the low pressure (LP) compressor, the influence of surface roughness in the HP compressor is more noteworthy.

**Other geometric parameters.** Due to the limitation of structural strength and processing technic, filets at compressor blade root,

stator blade root, and tip are usually unavoidable. The fillet will affect flow separation [33], and it has been shown that the addition of fillet can suppress the original stall condition [34]. The fillet radius also has a small effect on the hub loss. In addition, the geometry of the leading-edge fillet was found to have no effect on loss although there is usually visible manufacturing error in the leading edge [35].

In addition, the increase of leakage flow through stator shroud seals or rotor dovetails will also decrease compressor efficiency [36].

**2.1.3 Turbine.** In turbines, the geometric characteristics, manufacturing process, and internal flow characteristics are very different from those of fans and compressors [10]. The internal flow in a turbine is primarily a positive pressure gradient and complicated cooling systems are usually adopted in turbine blades. In turbines, manufacturing uncertainties may be the main cause of the large variety of turbine life [37].

Researches on the manufacturing geometrical uncertainty of the turbine are mainly categorized into two types: some researches focus on the performance variation with blade shape uncertainty, while many studies have focused on the effects of cooling system geometry on performance and life.

**Blade tip fillet and tip clearance.** Flow conditions in the turbine blade tip clearance region have an important impact on overall flow loss and blade tip heat loading. Figure 3 shows the influence of blade tip fillet radius  $r$  and tip clearance  $G$  on leakage mass flowrate  $M$  and tip heat loading  $H$ , which is obtained by simulation of a HP turbine [38]. It is indicated from Fig. 3 that when the tip clearance is doubled (from 0.75% to 1.5% span), the leakage flow will increase by 70%. Also, the leakage flow increases rapidly with the fillet radius. The increase in  $M$  will enhance leakage vortices and stage losses.

**Blade surface roughness.** The surface treatment process of a blade may lead to excessive surface roughness, which causes performance degradation [30]. Thermal barrier coatings can increase surface roughness by 10 times and may lead to severe loss. Specifically, the degree to which performance is affected varies with the Reynolds number [39]. To reduce roughness and improve efficiency, new coating technology or polishing [39] can be adopted.

**Cooling hole shape.** The cooling hole is very important for turbine cooling efficiency and life. However, as the sizes of cooling holes are usually very small, manufacturing uncertainties/defects are apt to occur. Therefore, many studies have focused on the manufacturing variations of cooling holes.

Laser drilling is a common method to produce film cooling holes, which is a fast but rough process and can result in irregular holes [40]. Defects in film cooling holes can be relatively large and reach 25% of the hole diameter [41]. The influence of cooling hole uncertainty varies under different velocity ratio [40]. In addition, under the same condition, the defect in the depth of the hole has no visible effect while that near the leading edge or outlet of the hole has a larger influence on cooling efficiency. What's more, Moeckel et al. [37] studied the effect of cooling hole diameter at

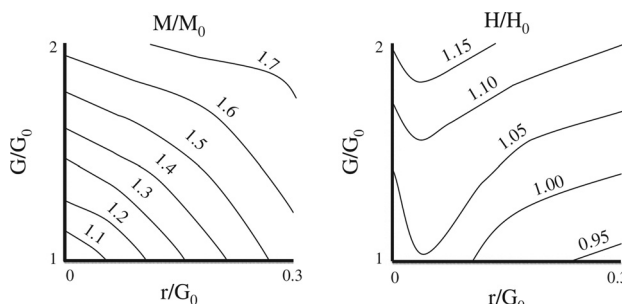


**Fig. 3 Leakage mass flow and heat loading under different geometric parameters [38]**

different locations. The results show that the diameter of the hole on the pressure side and near the trailing edge has the greatest influence on the blade section average temperature, which in turn affects the creep failure rate.

**Cooling hole surface roughness.** With the development of additive manufacturing (AM) technology using metal powder, gas turbine component manufacture by AM has achieved more and more attention. However, the parts produced by the current metal additive manufacturing technology have a large surface roughness, which is especially difficult to be smoothed in small internal passages.

Additive manufacturing for turbine blade will induce shape uncertainties in the cooling hole (surface roughness and flow area uncertainties, as shown in Fig. 4) [42]. When the hole diameter is small, it is almost completely blocked, while when the hole diameter is large, the relative roughness is reduced and the influence is reduced. In addition, the impact varies with the build direction of the cooling holes, as described in Ref. [42]. Further research shows that reduction of flow area will lead to lower coolant flow-rate, while the surface roughness will affect the overall cooling efficiency significantly by influencing film cooling, in-hole convection and internal convection [42]. To reduce the roughness, different materials can be used in AM according to Ref. [43].

**Summary of parameters.** Bunker [44] systematically summarizes the impact of manufacturing tolerances on turbine cooling performance and presents a summary of the typical manufacturing factors affecting turbine cooling, including the blade and cooling system geometry. More details can be obtained in Ref. [44].

Furthermore, Bunker using a simplified airfoil cooling model to evaluate the impact of several geometric parameters on the maximum turbine metal temperature in typical manufacturing tolerances and the Pareto diagram obtained is shown in Fig. 5. As can be seen from the figure, the film cooling geometry is the most significant, in which the film hole diameter and the length-to-diameter ratio  $L/D$  are the most influential coefficients whose manufacturing tolerance may make the maximum turbine metal temperature increase by 40 K. However, according to Ref. [44], 20 K increase in metal temperature may reduce the blade life by nearly 33% in severe conditions. According to Ref. [45], if the blade surface metal temperature deviates from the predicted value by 25 K, the blade life can be halved. This highlights the importance of considering the geometrical uncertainty in the overall life of turbines in the design process.

**2.2 In-Service Geometric Uncertainty.** During the gas turbine engine in-service period, due to corrosion, erosion, oxidation, fouling, and other factors, geometric uncertainty and performance deterioration will occur in compressors, fans, and turbines, which may significantly increase fuel consumption and operating costs. Performance deterioration phenomena of gas turbines are mainly divided into the following three types [46]: (1) recoverable deterioration: can be removed during gas turbine operation period; (2) nonrecoverable deterioration: not removable during engine operation but recoverable during overhaul; (3) permanent deterioration: residual degradation even after overhaul.

There are many studies on gas turbine component degradation and overall performance decrease [47]. Analysis based on JT3D and JT8D turbofan engine performance degradation data show that 60–70% of the observed increase in engine fuel consumption is caused by the deterioration of the fan and compressor, while 10–15% is due to turbine deterioration and the rest is related to the engine seal and clearance [47]. Also, because of the difference between the working medium constituent and the thermodynamic state in fan, compressor, and turbine, the inducement of performance degradation and the impact are significantly different.

To quantify the in-service geometric uncertainty, the geometric uncertainty model can be constructed based on measured blade geometric data using a method such as the PCA. However, in

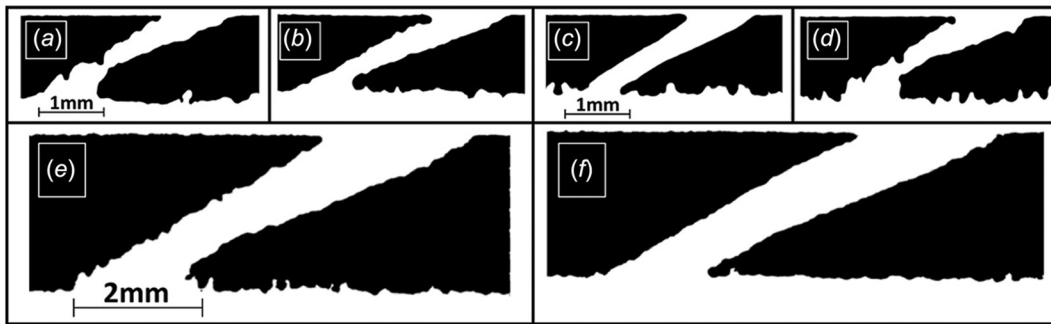


Fig. 4 Scan shape of cooling hole cross section by AM [42]

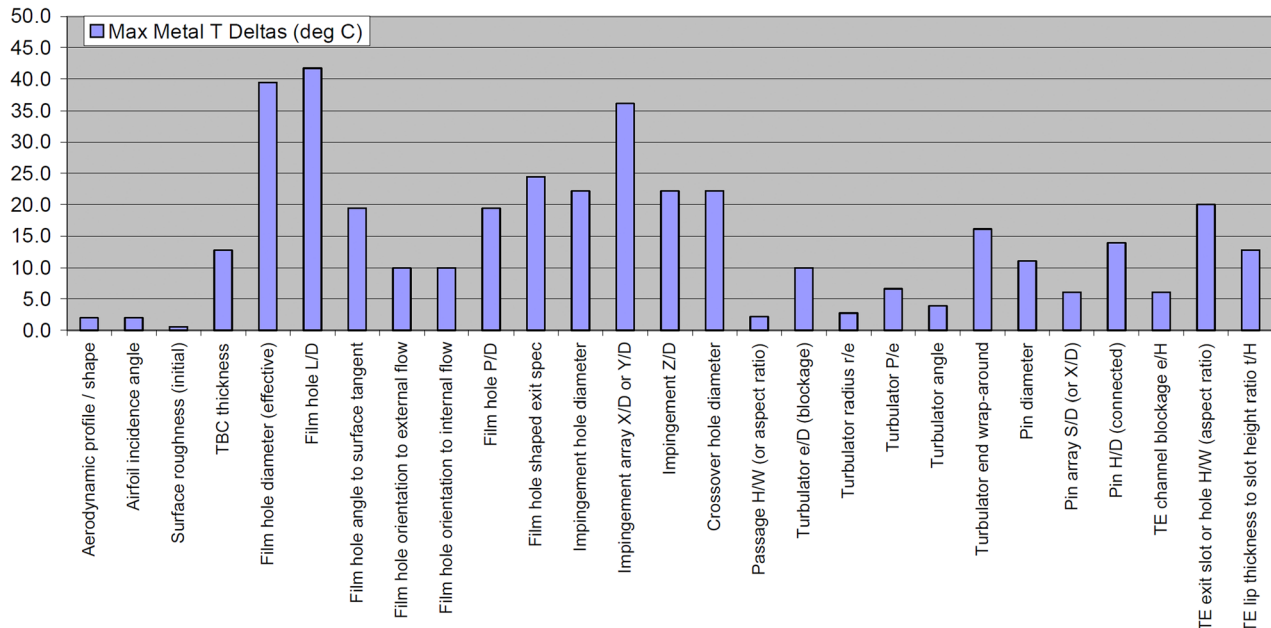


Fig. 5 Pareto chart of blade metal temperature deviation with manufacturing factors [44]

many studies, blade measured data are not available. In order to construct the geometric uncertainty models in such conditions, influential uncertainty variables with their corresponding statistical behavior can be determined based on available literature or experience [48,49]. Therefore, the primary geometry uncertainty variables resulting from different causes during operation are reviewed as follows.

**2.2.1 Fan.** When operating in a dusty environment, the fan blades are subject to aggressive particles, resulting in blade erosion and unrecoverable degradation in performance. Erosion of a fan can result in increased engine fuel consumption and reduced efficiency, mass flowrate, power, and surge margin [50].

The erosion pattern of the fan blade can be simulated by particle trajectory prediction [51], based on which the performance degradation and life prediction model of the fan under erosion conditions can be obtained [52]. Researches have indicated that the decrease in fan performance under erosion is mainly due to changes in blade leading/trailing edge shapes, reduction in chord length, increase in tip clearance, and surface roughness [52].

To improve the blade's resistance to erosion, the coating process can be applied based on a clear erosion pattern. Moreover, the degradation of eroded blade performance due to the leading-edge deviation and reduced chord length can be recovered by blade airfoil remodeling during overhaul [53]. On the other hand, the effect of the tip clearance variation due to erosion on the performance is also very significant. However, the standard repair

process corresponding to an increased clearance does not have any performance optimization potential.

**2.2.2 Compressor.** Over the past few decades, compressor in-service deformation effect on performance has been a major concern in a lot of studies. A study by Roberts [53] pointed out that compressor blade degradation may result in an increase in the thrust specific fuel consumption by 3% or more. In fact, a 0.5–1% fuel change could mean the difference between an aircraft operator's profit and loss [53].

The causes of compressor in-service degradation mainly include fouling, erosion, corrosion, and wear. Among them, fouling is a major form of recoverable degradation, while erosion, corrosion, and wear can cause unrecoverable degradation of the compressor [46].

**Fouling.** Fouling is a serious degradation phenomenon of compressors and a major form of recoverable degradation [46]. Compressor blade fouling can occur when there are factors such as airborne salts, industrial pollution, gas turbine exhaust, mineral precipitation, and so on. The blade fouling pattern can be obtained by experimental or analytical approaches [50]. Fouling can result in blade aerodynamic profile deterioration and hence loss of compressor flow capacity and efficiency, which in turn leads to rematching of the whole engine and reduced output power and thermal efficiency [54]. Moreover, compressor operating stability will also be affected: since fouling reduces the mass flowrate and increase the pressure ratio of the first stage of the compressor,

affecting the performance of the latter stages and reduces the flow coefficient of the second stage. This effect will continue for several stages until the surge is induced from the latter stages [55].

**Erosion.** Erosion means that the blade material is removed by hard particles such as gravel and dust. Erosion is not a major problem for industrial gas turbines due to the presence of air filtration systems, while in aircraft engines is serious because it is easy to inhale gravel, dust, water in the puddles, and so on when flying at low altitudes, taking off, and landing. Erosion can account for 45% of the total performance degradation of modern turbofan engines [46]. The blade fouling pattern can be obtained by experimental or analytical approaches [50]. The decrease in performance is mainly due to the leading-edge bluntness increase, trailing edge sharpening, chord length decrease, surface roughness increase, and tip clearance increase. In addition, significant loss of tip solidity may cause a compressor surge [50].

**Corrosion.** The deposits on compressor blades usually contain sodium chloride and potassium chloride, which can form an aggressive acid by combining with water and cause blade pitting corrosion [46].

Compressor pitting corrosion can significantly increase blade surface roughness [56] and enhance the turbulent flow in compressor [57], thereby reducing the compressor aerodynamic performance [58] or even leading to compressor stall in extreme cases [59].

**Wear.** Wear is a serious problem in the early operation periods of engines. It may be caused by thermal growth and centrifugal growth. Wear can lead to an increase in the clearances including tip clearance and sealing clearance, which is an irrecoverable deterioration. Tip clearance increase is a crucial reason for compressor efficiency decrease, which in turn leads to a decrease in engine power and efficiency. In addition, blade tip stall may also be caused by tip clearance increase. An increase in the seal clearance will cause a flow recirculation effect, which produces a similar effect to that of the tip clearance.

For compressor in-service degradation problems, protective coatings can be applied, such as corrosion-resistant coating, anti-oxidation coating, and fouling resistant coatings [60]. However, it is worth noting that the coating application process itself can introduce geometric and performance uncertainty as well, more details can be seen in Sec. 2.1.2.

**2.2.3 Turbine.** Different from fan and compressor, the turbine is a hot end component and the temperature of the internal working fluid is very high. Therefore, the turbine in-service degradation phenomena not only include fouling, erosion, and corrosion, but also include specific problems in hot end components such as high-temperature oxidation, sulfurization, and hot corrosion.

**Fouling.** Although fouling is mainly present in cold-end components, it may also occur in the turbine. Pollutants that cause the turbine fouling can enter the gas turbine through influent air, liquid fuel, fuel additives, or  $\text{NO}_x$  controlled injection fluid. Within the turbine, some ash, metals, and unburned hydrocarbons with a low melting point are deposited due to a drop in static temperature. Fouling will increase blade surface roughness, and thus result in the changes of boundary layer transition and increased losses. In addition, the thermal load of the turbine blade will be further increased and the blade metal wall temperature and life will be affected, which in turn will result in reduced overall engine efficiency [61], increased fuel consumption and increased exhaust gas temperature [62]. In addition, fouling on the turbine guide vanes may change the throat area, affecting the compressor-turbine match and causing the matching points to deviate from the design point, and thus results in performance degradation. Furthermore, the blade and disk cooling system can also be affected by fouling, resulting in reduced component life or even component failure.

**Erosion.** Erosions in the turbine involve particle erosion and hot gas erosion. Solid particles are inevitably ingested during gas turbine

operation [63]. The erosion caused by particulate matters will affect the aerodynamic performance and cooling performance of the turbine by changing the blade surface roughness, the turbine vane throat area, and the cooling hole flow area. On the other hand, hot gas erosion usually appears when there is intermittent cooling insufficiency or when the blade coating is broken, and it will influence turbine performance by affecting surface roughness [46].

**High-temperature oxidation, sulfuration, and hot corrosion.** When the surface temperature of the nickel-based super-alloy is reached to  $538^\circ\text{C}$ , the alloy will react with the oxidation and high-temperature oxidation will occur. The oxide layer will tend to be broken when the engine starts, stops, or vibrates. This phenomenon will affect the blade surface roughness or the cooling hole flow area [46].

In addition, there may be sulfide coming from fuel combustion flow into the turbine, react with the blade surface protective layer and produce highly corrosive  $\text{Na}_2\text{SO}_4$  slag, which is a sulfuration phenomenon. At high temperatures, the protective layer under the slag will be destroyed. Especially, when there appears sulfuration in the blade end-wall region or leading/trailing regions, there might be significant influence [46].

Hot end components are usually faced with combined oxidation and sulfuration problems, which is known as hot corrosion [46]. Turbine hot corrosion can be divided into two categories: among  $825\text{--}950^\circ\text{C}$ , the blade base metal may be removed, while in  $700\text{--}800^\circ\text{C}$  a layered corrosion scale appears [64].

**High-temperature creep.** Due to the high temperature in the turbine, the first-stage guide vane is susceptible to creep deformation, which in turn causes a change in the throat area. In most cases, the area will increase. The uncertainty in the throat area will change the compressor-turbine match and the operating line, as shown in Fig. 6, and thus, the aerodynamic performance or operating stability will be affected [46].

**2.3 Summary of Geometric Uncertainty Influencing Factors.** The main sources of geometric uncertainty variables that affect the performance vary significantly in different components due to the differences in their geometric and operating environmental characteristics. Montomoli et al. [4] summarize the influence of geometric uncertainties from different sources (manufacturing, in-service, and unknown sources) on several performance parameters (efficiency, stability, work, and life) in different components of a turbofan, as in Fig. 1.

Based on the review of Fig. 1, Secs. 2.1 and 2.2, the predominant geometric uncertainty factors of each component can be summarized as follows:

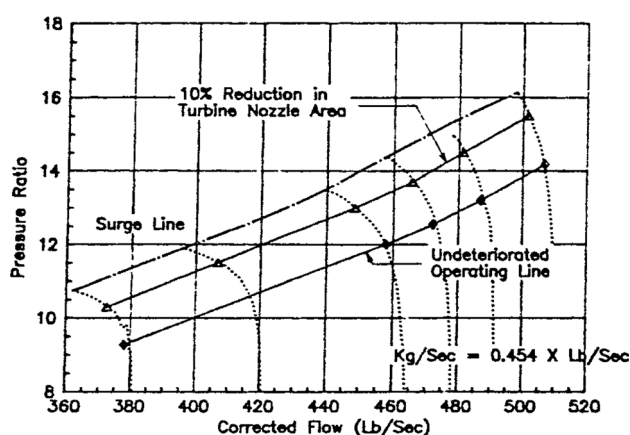


**Fig. 6 Effect of turbine guide vane throat area on the operating line of gas turbine [46,65]**

**2.3.1 Fan.** The performance of a fan is mainly affected by the in-service uncertainty and is also affected by the manufacturing uncertainty. In-service geometric degradation factors mainly include leading/trailing edge shapes change, chord length reduction, tip clearance increase and surface roughness increase caused by particle intake erosion. These factors may lead to a decrease in fan efficiency and flowrate, thus resulting in a decrease in overall engine efficiency and work. As for manufacturing uncertainty, the leading-edge shape change or seal leakage increase may lead to significant performance reduction.

**2.3.2 Compressor.** The performance of the LP compressor is affected by both manufacturing and in-service uncertainty, while the performance of the HP compressor is mainly affected by the manufacturing uncertainty due to its small size.

On the one hand, as for manufacturing uncertainty, blade leading-edge shape change, tip/seal clearance increase, surface roughness increase, fillet radius change are the predominant factors and may lead to a reduction of the engine efficiency, stability, and work. As for in-service uncertainty, the performance deterioration is mainly due to nozzle area decrease, leading-edge bluntness increase, trailing edge sharpening, chord length decrease, surface roughness increase, and tip/seal clearance increase.

**2.3.3 Turbine.** The HP turbine performance is mainly affected by manufacturing uncertainty and also affected by the in-service uncertainty, while the LP turbine performance is virtually affected by neither manufacturing nor in-service uncertainties according to Fig. 1.

On the one hand, as for manufacturing uncertainty, the increase of blade tip clearance or surface roughness may reduce the aerodynamic efficiency, thereby reducing overall engine efficiency and work. Also, the manufacturing uncertainty of cooling systems such as the increase of film hole diameter and the increase of cooling hole surface roughness may lead to serious cooling performance deterioration and hence service life reduction. On the other hand, as for in-service uncertainty, factors that cause performance deterioration mainly include the increase of blade surface roughness, the change of turbine vane throat area, and the decrease of cooling hole flow area.

### 3 Geometric Uncertainty Quantification Method

As the deterministic simulation method cannot take into consideration the influence of geometric uncertainty factors [4], a large number of researches have been conducted to develop different UQ methods to quantify this influence [5]. The purpose of this section is to give an overview of the UQ process and introduce the principles of different UQ methods adopted in the gas turbine field.

**3.1 Uncertainty Quantification Process.** The typical UQ analysis schematic is presented in Fig. 7. The first step is uncertainty definition, which means to determine the distribution of the uncertainty input variable  $X$ , which can be obtained through experiments [66] or expert opinions and is usually expressed by the probability density function (PDF). The next step is uncertainty propagation, which means to determine the distribution of response variable  $Y$ , based on the distribution of  $X$ , and the model defining the quantitative relation between  $X$  and  $Y$ . Finally, the uncertainty certification is conducted to evaluate the confidence

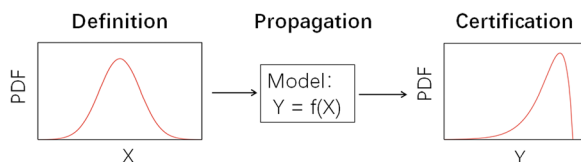


Fig. 7 UQ analysis schematic

coefficient of the quantification results by comparing the distribution of  $Y$  obtained from UQ simulation and that from experiments. Then, a series of uncertainty analyses, such as reliability evaluation, can be carried out based on the quantification results [4].

The UQ methods applied to gas turbines mainly include the sampling-based method, sensitivity-based method, surrogate model-based method, and PC method, which will be reviewed separately below.

### 3.2 Principle of Uncertainty Quantification Methods

**3.2.1 Sampling-Based Method.** The sampling-based method quantifies the influence of uncertainty by conducting stochastic simulation and is the most straightforward UQ method. The Monte Carlo (MC) method is one of the most extensively applied sampling-based methods due to the simple principle [6].

The basic idea of MC method is [6]: a pseudo-random sampling of independent random variables vector  $\xi$  is conducted to build a set of samples of input stochastic variables  $\{X^1, X^2, \dots, X^N\}$ , wherein  $X$  is the independent random variable vector and  $X \equiv X(\xi)$ ,  $N$  is the number of samples. Each sample corresponds to a unique solution  $Y^i \equiv Y(\xi^i)$ ,  $i = 1, 2, \dots$ , which can be determined by the system model  $M(Y, X) = 0$ . The collection  $\{Y^1, Y^2, \dots, Y^N\}$  is called a collection of sample solutions, based on which the statistical characteristics of  $Y$  can be estimated. For example, the mathematical expectation  $\hat{Y}$  and variance  $\sigma_Y^2$  can be evaluated according to the following formula:

$$\hat{Y} = \lim_{N \rightarrow \infty} \frac{1}{N} \sum_{i=1}^N Y^i \quad (3.1)$$

$$\hat{\sigma}_Y^2 = \frac{1}{N-1} \sum_{i=1}^N (Y^i - \hat{Y})^2 \quad (3.2)$$

where  $\partial_i$  is the relative weight of the sample  $i$ , and  $\sum_{i=1}^N \partial_i = N$  (for unbiased sampling,  $\partial_i \equiv 1$ ).

The MC method is not only simple but also very robust [67], as it does not require any assumptions or conditions about the variance of the input variables, the regularity of  $Y(\xi)$  or the form of the model. However, the MC method requires a high-fidelity model which might be expensive to solve in complicated problems. In addition, the samples are not spatially filled essentially [68], which results in a slow convergence rate  $O(\sigma_Y N^{-1/2})$  [6]. In response, some improved methods have been developed, such as the quasi-Monte Carlo (QMC) method which can converge faster at a rate of  $O(\ln N^d / N)$  [6] (as shown in Fig. 8).

**3.2.2 Sensitivity-Based Method.** The sensitivity-based methods describe uncertainty propagation by using the derivative of the objective function, i.e., the sensitivity derivative. The basic idea of this method is: first, the sensitivity derivative is obtained by difference methods or solving input-output correlation

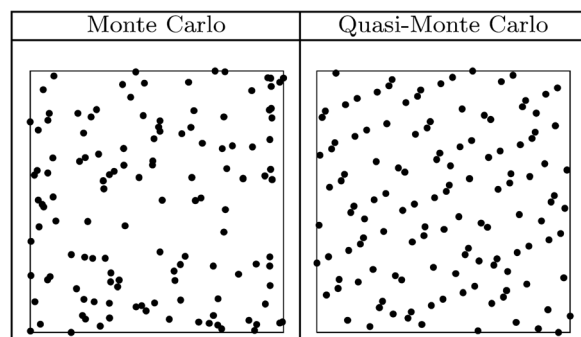


Fig. 8 Pseudo-random sample set of the MC and QMC methods on a unit square ( $N = 128$ ) [6]

equations. Second, the approximate function between  $Y$  and  $X$  is constructed based on the sensitivity derivative, or the random space dimension reduction is performed, and then the UQ analysis can be carried out.

Sensitivity derivatives can be calculated by the finite difference method, tangent linear method, or adjoint method [69], among which the adjoint method is the primary focus in researches due to the high efficiency and high precision of sensitivity calculation [70]. Its basic principle is: first, the flow control differential equation is adopted as a constraint, and then the adjoint operator is used to introduce the variation of the flow equation into the variation of the response variable  $Y$ . By eliminating the influence of the flow field variation on the variation of the response variable  $Y$ , the adjoint equation and the corresponding sensitivity can be determined. Define the response variable  $Y$

$$Y = Y(\omega, X) \quad (3.3)$$

where  $\omega$  is the flow field variable, and  $X$  is the geometric variable. Variation of the  $Y$  is

$$\delta Y = \frac{\partial Y}{\partial \omega} \delta \omega + \frac{\partial Y}{\partial X} \delta X \quad (3.4)$$

The flow control equations  $R$  meet the condition:

$$R(\omega, X) = 0 \quad (3.5)$$

Its variation is

$$\delta R = \frac{\partial R}{\partial \omega} \delta \omega + \frac{\partial R}{\partial X} \delta X = 0 \quad (3.6)$$

Introducing adjoint operator  $\Psi$  and combining the Eqs. (3.4) and (3.6), there is

$$\delta Y = \left\{ \frac{\partial Y}{\partial \omega} - \Psi^T \frac{\partial R}{\partial \omega} \right\} \delta \omega + \left\{ \frac{\partial Y}{\partial X} - \Psi^T \frac{\partial R}{\partial X} \right\} \delta X \quad (3.7)$$

If the first-term coefficient in the right end of Eq. (3.7) is zero, the influence of the flow field variation on the variation of the objective function can be eliminated, thereby determining the adjoint equation and sensitivity  $\mathcal{G}$ , as shown in the following equations, respectively

$$\frac{\partial Y}{\partial \omega} - \Psi^T \frac{\partial R}{\partial \omega} = 0 \quad (3.8)$$

$$\mathcal{G} = \frac{\delta Y}{\delta X} = \frac{\partial Y}{\partial X} - \Psi^T \frac{\partial R}{\partial X} \quad (3.9)$$

It can be known from Eq. (3.9) that after determining the flow field and the adjoint field, it is only necessary to disturb the geometric boundary variable and realize the grid variation for the calculation of the sensitivity. Therefore, for each response variable  $Y$ , all the sensitivity information can be determined by solving the flow control equation and adjoint equation only once. So, it is very effective as the sensitivity calculation time is independent of the random space dimension  $d$ .

After obtaining the sensitivity derivative, the perturbation method can be used to construct an approximate correlation between  $X$  and  $Y$  using a first or second-order truncated Taylor series. The probability distribution of  $Y$  is approximated by the probability distribution of its low-order approximation and can be calculated directly based on the probability distribution of  $X$  [71]. This method is simple and effective and can significantly reduce the computational resources required [69]. However, its main disadvantage is the limitations in nonlinear correlation capture, i.e., the method is usually only applicable to small input variable biases because only in such conditions the

response variables can be considered to vary linearly with input variables [8].

Moreover, the sensitivity derivative can also be used to identify uncertainty variables with a significant impact on performance and reduce the dimension  $d$  of the random uncertainty space. Then, other UQ methods such as MC can be used to implement more accurate UQ analysis considering only the critical variables [72]. This method is the most suitable when the dimension  $d$  is large and the magnitudes of the uncertainty influence are only large for a small number of random parameters.

**3.2.3 Surrogate Model-Based Method.** To reduce the computational cost while maintaining the accuracy, the surrogate model-based methods have been developed as a low computational cost alternative to the original high-fidelity model for the sampling-based method [68]. The basic idea of the surrogate model-based method is: by analyzing the initial sampling set, to construct an approximate surrogate model  $\hat{Y} = \hat{f}(X, C) \approx f(X)$ , which is easier to compute than the original high-fidelity model  $Y = f(X)$ . In the equation,  $C$  is the undetermined coefficient vector to be estimated from the initial sample set.

The techniques for constructing surrogate models mainly include response surface models (RSM) [73], neural networks [74], support vector regression (SVR) models [48], and Gaussian stochastic process models [75]. RSM is a simple and extensively applied surrogate model. The RSM can be constructed by the design of experiment and interpolation or regression techniques [73]. A set of initial training datasets obtained by the design of experiment techniques and high-fidelity model simulations is represented by  $(X^{(i)}, Y^{(i)}, i = 1, 2, \dots, N)$ , and the quadratic RSM of  $Y$  can be expressed as

$$\hat{Y} = C_0 + \sum_{1 \leq j \leq p} C_j X_j + \sum_{1 \leq j \leq p, k \geq j} C_{j(p-j+2)+k-1} X_j X_k \quad (3.10)$$

where  $C_0, C_j, C_{j(p-j+2)+k-1}$  are the undetermined coefficients which can be estimated by interpolation or regression. Once the undetermined coefficient is determined, the output value  $Y$  can be directly determined by the RSM and the input vector  $X$ .

The surrogate model-based method can significantly reduce the amount of simulation required, greatly shortening the computation time and resources required for UQ analysis, and have significant advantages in the UQ application in a complicated system. However, some major problems faced by this method include the computational resources required to obtain the initial sampling set and construct the surrogate model, and the UQ analysis error that may be introduced by the difference between the surrogate model and actual input-output correspondence.

**3.2.4 Polynomial Chaos Method.** The PC method is one of the most widely used methods for UQ analysis through CFD models. The PC method is based on the homogeneous chaos theory [76], and the basic idea is to decompose the random variable into separable deterministic and random components and project the variables onto a random space with a set of completely orthogonal polynomials  $\Phi_i(\xi)$  as the basis [77]. Specifically, the response variable affected by random variables can be expressed as

$$Y = \sum_{i=0}^P c_i \Phi_i(\xi) \quad (3.11)$$

where  $c_i$  is the undetermined coefficient which represents the fluctuation amplitude of the  $i$ -th mode;  $\Phi_i(\xi)$  is the random basis function corresponding to the  $i$ -th mode, and according to the Askey scheme [77], there are different optimal polynomials  $\Phi_i(\xi)$  for different PDFs of input variables; and  $P = \frac{(d+p)!}{d!p!}$ , is a function of the PC expansion order  $p$  and random dimension  $d$ . By solving the undetermined coefficient  $c_i$ , a complete input-output function

can be obtained and the statistical features of  $Y$  can be evaluated by

$$E[Y] = c_0 \quad (3.12)$$

$$\text{Var}[Y] = \sum_{i=1}^P [c_i^2 \langle \Phi_i^2 \rangle] \quad (3.13)$$

When determining  $c_i$ , according to whether the govern equation solver (such as CFD solver) needs to be modified, the PC method can be divided into intrusive polynomial chaos (IPC) and nonintrusive polynomial chaos (NIPC) methods.

The random Galerkin method is a typical IPC method [78]. Since the new PC equation has different characteristics from the original governing equation and is usually more complicated, a new CFD solver is needed. Under certain conditions, it has been proved that the error of the  $p$ -th order truncated expansion decreases exponentially as the polynomial order  $p$  increase and is more efficient than the MC method while maintaining high precision [79]. However, the intrusiveness of IPC will bring a lot of inconveniences. First, when modifying the CFD solver, a lot of coding work is needed for complex engineering problems. Also, numerical instability may occur if the new equation is not properly discretized [80]. These two barriers have limited the application of IPC to complex problems.

In response to these limitations, the NIPC methods have gained attention for the applicability of commercial CFD solvers. It can be considered as a combination of the PC and sampling methods. The basic idea is to estimate  $\alpha_i$  based on the deterministic solutions of some samples, during which the CFD solver can be used as a black box of uncertainty propagation [81]. The probability collocation method [82] is an extensively used NIPC method, which uses the collocation method instead of random sampling to improve the convergence efficiency. In addition, it is applicable to any input distribution and converges exponentially with the polynomial order [82]. What's more, it is necessary to determine the probability distribution for all the input uncertainty variables before PC research. This might be very difficult in gas turbines because the collection of geometric uncertainty data is usually difficult and expensive, and thus scarce data are usually faced in UQ researches. In response, a new method called the sparse approximation of moment-based arbitrary polynomial chaos (SAMBA PC) has been proposed [83]. This method uses statistical moments as a quantitative measure of a random sample set or a PDF, which has been proved to be able to provide accurate analysis results for scarce datasets.

The PC method has been proved to be superior for fast convergence and high precision in low-dimensional uncertainty problems, but the method still has the limitation named “curse of dimensionality”: the cost of solving the PC expansion coefficient is at least proportional to the number of terms  $P$  in expansion equation [84] and thereby usually increases exponentially with respect to the number of dimensions  $d$  as  $P = \frac{(d+p)!}{d!p!}$ . In complex problems,  $d$  may be hundreds or even thousands, making the PC method completely infeasible [70].

## 4 Geometric Uncertainty Quantification Application in Gas Turbine

As the performance and reliability requirements of gas turbines increase continually, more and more researches have focused on the UQ researches in the gas turbine. By conducting UQ study, the distribution features of the gas turbine performance can be obtained and reliability evaluation can be carried out [1,2], the key geometric parameters that affect performance can be distinguished [1,3], and tolerance optimization [3] and blade robust design optimization can be conducted [2].

The purpose of this section is to give a review of existing UQ researches using different UQ methods, extract the characteristics

and applicable conditions of each method, and summarize the research progress and challenges remaining currently.

### 4.1 Sampling-Based Method

**4.1.1 Application in Fan/Compressor.** Based on the sampling-based method, the performance distribution under geometric uncertainties can be obtained. Schnell et al. [1] conducted sampling considering the first six eigenmodes of a rotor blade (which are obtained by PCA and shown in Fig. 2). In this study, it is assumed to be normally distributed for each eigenvector and about 1000 samples are generated. For each of the samples, the two-dimensional (2D) coupled Euler/boundary layer solver MISES [85] is applied to assess the aerodynamic performance of the blade section, and the results are shown in Fig. 9. Under different inflow angles, when the airfoil geometry deviates from the nominal value, the outflow angle presents a different uncertainty distribution [1].

Moreover, sensitivity analysis can be adopted based on the sampling results to identify the key geometric uncertainty variables in gas turbines. Lange et al. [86] investigated the sensitivity of 18 manufacturing geometric variables in a 1.5 stage HP compressor blade by CFD simulations of 500 samples. The Spearman rank correlation coefficient  $r$  is chosen to quantify the sensitivity of performance to geometric variables. The results are shown in Fig. 10, indicating that the leading-edge thickness has the largest effect on efficiency, while the stagger angle is the most influential to the blade turning.

**4.1.2 Application in Turbine.** To quantify the impact of the blade manufacturing geometric uncertainties on performance, Duffner [87] conducted MC sampling based on the PCA results of a transonic turbine vane and each sample is simulated by 2D solver MISES. Based on the samples, sensitivity analysis indicates that the flow condition is almost insensitive to geometric uncertainties at the upstream of the throat while it is more sensitive to the throat and trailing edge geometry.

In addition, as for the geometric uncertainty of the turbine cooling system which is also very important, Bunker [44] uses the MC method combining with a one-dimensional (1D) blade cooling model to analyze the effect of blade film cooling manufacturing uncertainty on the distribution of blade metal temperature. The result is shown in Fig. 11 and indicates that the manufacturing uncertainty of the film cooling holes may cause the blade surface metal temperature to fluctuate within the range of  $\pm 20^\circ\text{C}$ . However, a  $20^\circ\text{C}$  increase of metal temperature may result in a

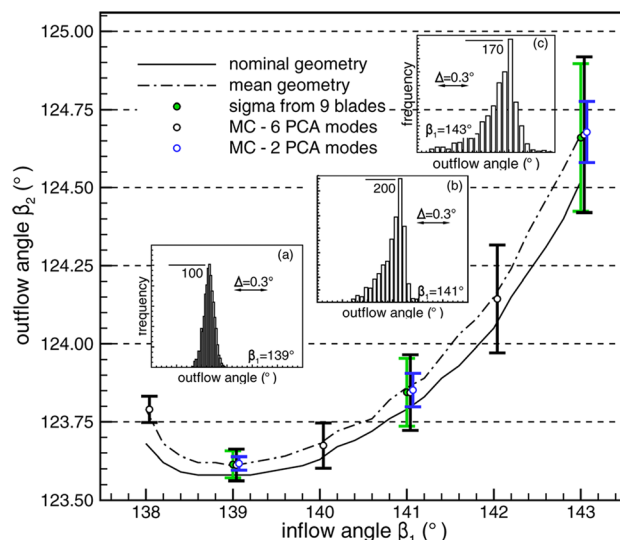


**Fig. 9 Outflow angle  $\beta_2$  distribution under geometric uncertainties at different inflow angles  $\beta_1$  [1]**

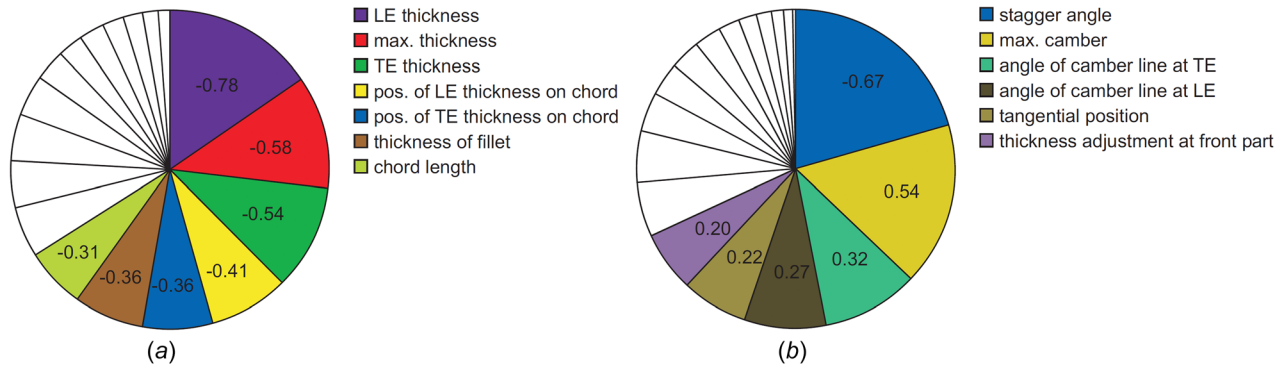


**Fig. 10 Sensitivity of HP compressor performance parameters to blade geometric variables [86] (a) sensitivities of isentropic efficiency and (b) sensitivities of blade turning**

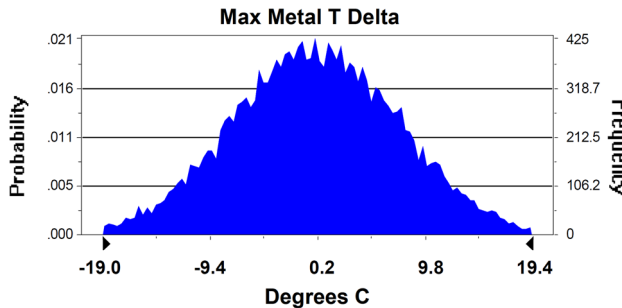


**Fig. 11 Blade metal temperature distribution [44]**

reduction of approximately 33% in blade life. Therefore, the potential impact of cooling hole uncertainties must be considered when determining the manufacturing tolerances.

In conclusion, UQ analysis by sampling-based methods can be used to predict the performance distribution under geometric uncertainties or identify the critical variables, based on which tolerance optimization can be implemented [3]. However, due to the slow convergence rate and the application of higher-fidelity computational models, it is still very expensive with a large number of samples to be simulated when applied in gas turbines [6].

## 4.2 Sensitivity-Based Method

**4.2.1 Application in Fan/Compressor.** The adjoint method is capable of efficiently calculating the sensitivity of the

performance variable to a large number of geometric variables. Tang et al. [88] use an adjoint solver to obtain performance sensitivity to geometric uncertainty along the entire blade surface in NASA Rotor 67 compressor. The result is shown in Fig. 12, which indicates that the blade performance is most sensitive to the central region of the blade suction surface.

It is worth noting that the applicable range of the method must be considered. Giebmans et al. [8] studied the applicable scope by comparing the results of the adjoint method and nonlinear CFD simulation. It is indicated that the method can predict performance variation accurately under small-scale geometric variation. However, it can only give the performance change trend but cannot be used for quantitative prediction in larger variation range, as shown in Fig. 13, wherein  $F$  is the sensitivity of the response variable,  $\delta\epsilon$  is the geometric variable deformation value and [-] represents unit of 1.

In conclusion, the sensitivity-based method is most efficient but it is only suitable for problems with small uncertainty variation ranges because it has difficulty in capturing nonlinear relationships in larger variations.

## 4.3 Surrogate Model-Based Method

**4.3.1 Application in Fan/Compressor.** The surrogate model can be used to predict the response variable value rapidly, which can significantly reduce the CFD computational resources required in UQ process. He and Zheng [74] adopted the artificial neural network (ANN) as a surrogate model and the fast prediction of the performance in a high pressure ratio centrifugal compressor under ten geometric uncertainty variables. Based on the

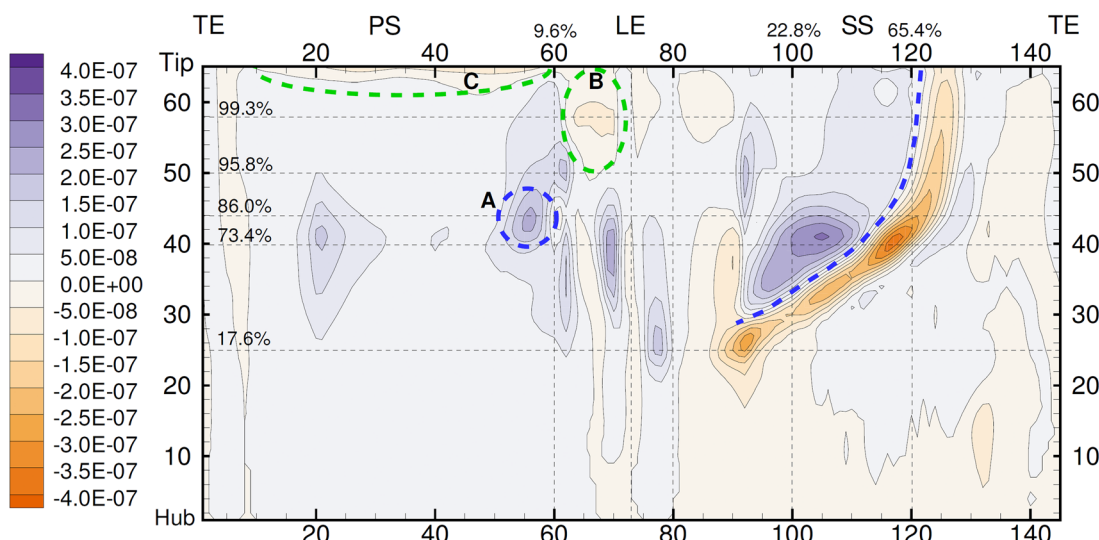


**Fig. 12 Adjoint sensitivities to blade surface geometric parameters [88]**

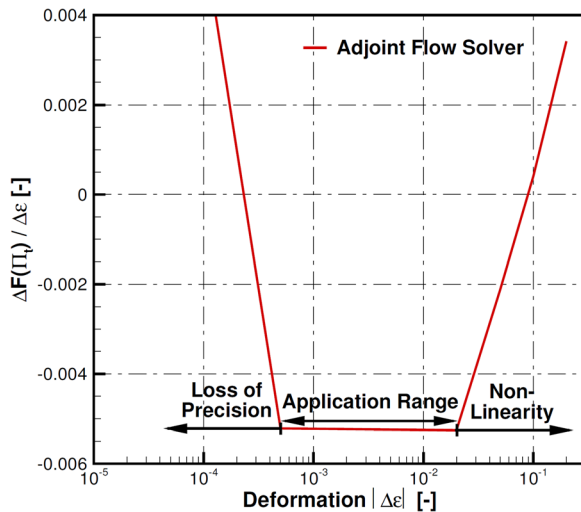


Fig. 13 Estimated applicable range of the adjoint solver [8]

ANN model, on the one hand, the key parameters can be identified. In this study, the key parameters are the camber curve shape in the blade tip section near the leading edge and the blade stacking line shape close to the end-wall region. On the other hand, the ANN model is combined with the genetic algorithm, which greatly reduces the calculation amount required for the complex three-dimensional geometry optimization of the compressor and achieves performance improvement.

However, it is worth noting that the computational cost required for building an exact surrogate model may increase exponentially with the number of dimensions  $d$  of the geometric uncertain variables. This limits the application in high-dimensional UQ problems to a large extent. Therefore, the sensitivity analysis can be used to identify the least significant geometric variables and fix them to the nominal values, thus reducing the number of dimensions  $d$ . For example, the active subspace method is proposed [75]. Qin et al. [49] adopt the active subspace method to simplify the original eight-dimensional problem to a one-dimensional problem and constructed a low-order SVR model. The model is verified by the CFD calculation results of 48 samples and results show that it can reflect the geometric-performance correspondence to some extent, but there are still some deviations (Fig. 14).

**4.3.2 Application in Turbine.** The surrogate model-based method can be applied to performance/reliability assessment or

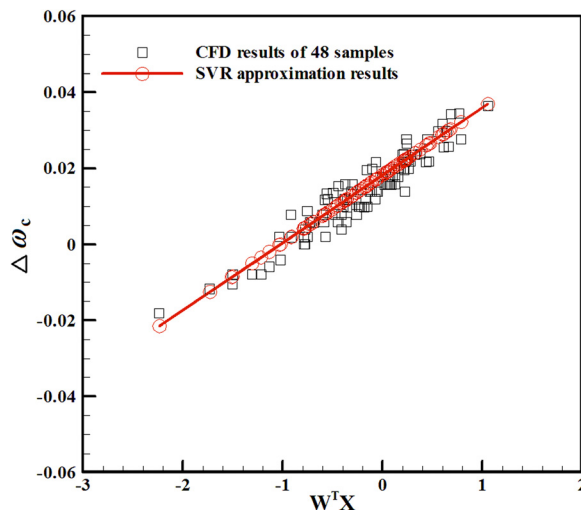


Fig. 14 Comparison of low-order SVR surrogate model and CFD simulation results [49]

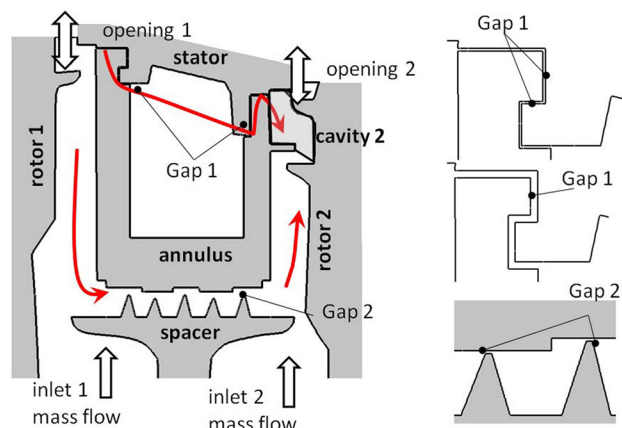


Fig. 15 Schematic of the interwheel cavity in a LP turbine [66]

probabilistic evaluation of blade failure or even serious accidents, which traditional design might be unable to detect [12]. Montomoli and Massini [66] studied the geometric uncertainties of interwheel cavities in a LP turbine using a surrogate model. Considering two geometric uncertainty variables: gaps 1 and 2 (Fig. 15), 25 CFD simulations are performed to build an RSM, as in Fig. 16.

Based on the RSM, the probability of exceeding the critical temperature has been investigated under different input distributions (as shown in Table 1) and indicates that when considering a probability distribution with “fat-tail,” the probability of exceeding the critical temperature could be improved by about four orders of magnitude, which means a much higher occurrence probability of the “black swan” event and the corresponding serious consequences. Therefore, it is important to select the distributions of input variables carefully during the reliability evaluation based on UQ analysis.

In conclusion, the surrogate model-based method can decrease the computational cost while maintaining the accuracy of UQ result. The disadvantage is that the computational cost required to build a precise surrogate model can be very high in high-dimensional problems.

#### 4.4 Polynomial Chaos Method

**4.4.1 Application in Fan/Compressor.** In recent years, with the continuous increase of the number of dimension  $d$  in UQ

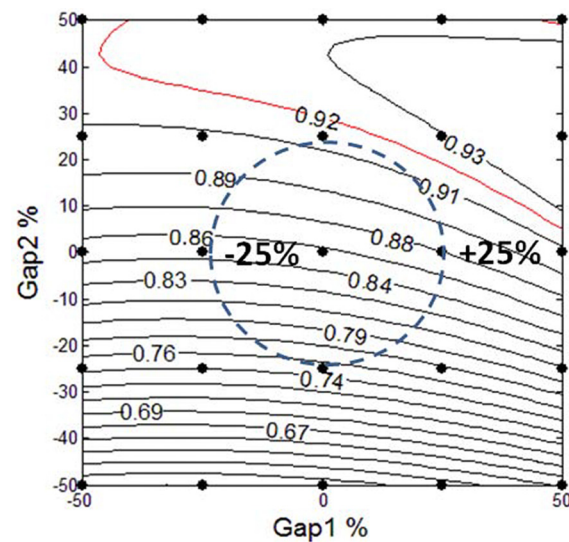


Fig. 16 Surrogate model for performing UQ analysis [66]

**Table 1 Probability of the response variable exceeding a critical value under different input distributions [66]**

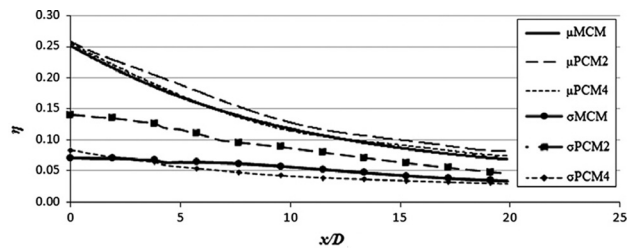
	$P(T > T_{\text{crit}})$
Gauss PDF	$2.54 \times 10^{-4}\%$
Cauchy PDF	2.33%
$t$ -distribution, $\nu = 100$	$6.01 \times 10^{-4}\%$
$t$ -distribution, $\nu = 50$	$1.51 \times 10^{-3}\%$
$t$ -distribution, $\nu = 10$	$4.16 \times 10^{-2}\%$
$t$ -distribution, $\nu = 5$	0.24%
$t$ -distribution, $\nu = 3$	0.74%
$t$ -distribution, $\nu = 1$	3.22%

studies of gas turbines, an advanced sampling algorithm: sparse grid method has been combined with the PC method to reduce the required simulations while maintaining the UQ analysis accuracy by select appropriate samples. The required sample numbers of sparse grid method with linear and exponential growth in the 1D-level rules and the conventional full tensor grid method are compared in Table 2 and show that the sparse grid method can dramatically reduce samples needed.

Wunsch et al. [89] combine sparse grid method and PC method to study the effects of coexistence of operational and geometric uncertainties. This study is based on the NASA Rotor 37 transonic compressor, with up to nine uncertain variables (inlet total pressure, outlet static pressure, tip clearance, leading-edge shape and trailing edge shape, etc.). Based on the simulation results, the scaled sensitivity derivative can be used to identify the critical variables and the result shows that the blade leading-edge angle and tip clearance are the two geometric parameters that have the greatest influence on performance (total pressure ratio, mass flow-rate, and efficiency). In addition, the study has achieved full automation of the geometry modification and meshing process based on the commercial software NUMECA. This combination of automation and the introduction of sparse grid quadrature represents a breakthrough in the application of uncertainty management in engineering practice.

**4.4.2 Application in Turbine.** When the number of dimension  $d$  is less than 5, the PC method has been proved to be able to converge fast while maintaining an accurate statistical distribution of output variables. Figure 17 presented the statistical result (mean and standard deviation of adiabatic effectiveness) from Monte Carlo multilevel sampling method, second-order and fourth-order PC method, and it is indicated that fourth-order PC method based on 25 samples can give a comparable result compared with MC result based on 242 samples [90]. Moreover, a similar conclusion has been obtained by Ghisu et al. [91] validated under  $d = 3$ .

To overcome the limitations of sparse data, the SAMBA PC method is applied to turbine UQ studies and verified by Ahlfeld and Montomoli [83]. It is applied in the UQ study on manufacturing geometric uncertainty in a LP turbine, and the selected eight input variables along blade airfoil. Among the eight variables, the geometric data of the six sections are given in the form of

**Fig. 17 Statistics comparison for the MCMLS and PC second and fourth-order [90]**

frequency distribution histograms, while the geometric data of the two points are given in the form of continuous PDFs. This study demonstrated the SAMBA PC method's flexibility in the application in gas turbine UQ analysis with two kinds of input data forms. Moreover, the Sobol sensitivity indexes of different variables can be calculated based on PC expansion. The results show that although the geometric variation in the suction surface is small, its effect on pressure loss is greater than that in the pressure surface. In particular, the uncertainty of the third section contributes 85% of the total variance.

In conclusion, the PC method is most widely applied in UQ analysis in the CFD field, it has significant advantages of fast convergence and high accuracy in low-dimension UQ problems. However, it also faces a serious "curse of dimensionality" in high-dimensional problems.

## 5 Conclusions

In this paper, the geometric uncertainties along with UQ methods in gas turbines were comprehensively reviewed. First, the main sources and features of gas turbine geometric uncertainty are reviewed. Then, the basic principles, characteristics, and application of different UQ methods are reviewed. Based on the reviews above, the main conclusions are as follows:

The sources of geometric uncertainty in gas turbines mainly include manufacturing and in-service geometric uncertainty, which have different influence in different components:

- (1) The performance of a fan is mainly affected by the in-service uncertainty due to particle intake erosion.
- (2) The performance of a LP compressor is affected by both manufacturing and in-service uncertainty while the performance of the HP compressor is mainly affected by the manufacturing uncertainty due to the small size.
- (3) HP turbine performance is mainly affected by the manufacturing uncertainties of both blade profile and cooling system, while the LP turbine performance is virtually unaffected by both manufacturing and in-service uncertainties.

There are mainly four UQ methods adopted in gas turbines with different characteristics:

- (1) The sampling-based method is the simplest and extensively applicable. However, it might be very computationally

**Table 2 Comparison of sample numbers of a full tensor grid and a sparse grid [89]**

Level	0			1			2			
	Dimension	Tensor	Sparse LG	Sparse EG	Tensor	Sparse LG	Sparse EG	Tensor	Sparse LG	Sparse EG
1	2	1	1	1	3	3	3	4	5	7
2	4	1	1	1	9	5	5	16	17	21
3	8	1	1	1	27	7	7	64	31	37
4	16	1	1	1	81	9	9	256	49	57
5	32	1	1	1	243	11	11	1024	71	81
...	...	...	...	...	...	...	...	...	...	...
10	1024	1	1	1	59049	21	21	1,048,576	241	261

- expensive when the result precision required is high due to the slow convergence rate.
- (2) The sensitivity-based method is the most efficient method but it is only suitable for problems with small uncertainty variation ranges while it can only give information about the performance change trend in larger variations.
  - (3) The surrogate model-based method can significantly decrease the computational cost while maintaining UQ precision. The disadvantage is that the computational cost required to build a precise surrogate model can be very high in high-dimensional problems.
  - (4) Polynomial chaos method has significant advantages of fast convergence and high precision in low-dimension UQ problems. However, it also faces a serious “curse of dimensionality” in high-dimensional problems.

These methods can be selected to achieve a balance between research precision and efficiency considering practical research conditions or objectives.

The main challenges of geometric uncertainties quantification study in gas turbines include:

- (1) *Challenges in simulation precision:* As the geometric variation range in gas turbines is usually small, it is necessary to ensure the high precision of geometric modeling and numerical simulation to accurately reflect the geometric uncertainty and its impact on performance. Therefore, the simulation method adopted in UQ analysis gradually transitioned from 1D and 2D simulations to 3D CFD simulation, and in the future methods such as large eddy simulation or direct numerical simulation may also be applied to UQ analysis, which will continuously increase the computational cost.
- (2) *Curse of dimensionality:* A large number of geometric uncertainty variables often exist simultaneously in gas turbines, which will not only affect performance separately but also interact with each other, leading to combined effect. Therefore, the number of variables investigated simultaneously in UQ analysis gradually increases, leading to the exponential increase in the simulations required, which is the most important challenge in current UQ researches.

## 6 Recommendations

Based on the relevant frontier research, the future prospects of geometric uncertainty quantification research in gas turbines can be summarized as follows:

- (1) *Geometric uncertainty study considering the operational conditions:* It has been observed in many cases that the influence of geometric uncertainty on performance may be fundamentally different under different operating conditions (which can be represented by different Mach number, Reynolds number, or flow coefficient). Therefore, to categorize the geometric uncertainty influence in terms of operating conditions will be potentially meaningful to help understand the influence mechanism explicitly and instructive in the design and optimization of gas turbines.
- (2) *UQ method combined with the dimensionality reduction method:* To avoid the “curse of dimensionality,” it is important to limit the number of dimensions in the UQ study. Therefore, advanced dimensionality reduction methods can be adopted, which means identifying and eliminating the noncritical geometric variables, and thereby the random space dimensionality can be reduced. The dimensionality reduction methods can be mainly classified into two categories: dimensionality reduction based on physical mechanisms or mathematical algorithms. The dimensionality reduction based on physical mechanisms is to reasonably exclude the geometric variables that have less impact on

performance based on rich experience in gas turbine design and the influence rule and mechanism of geometric variables on performance. And as for the dimensionality reduction method based on mathematical algorithms, a typical method is the active subspace dimensionality reduction method, which uses sensitivity analysis to reduce the number of dimensions. In the future, advanced techniques such as data mining may also be combined to reduce computation costs.

- (3) *UQ method combined with the Artificial Intelligence algorithm:* There are usually hundreds of CFD simulations in UQ studies in gas turbines which cost a lot of computational resources and time. However, in the following UQ study or design optimization, only several performance indexes (such as mass flow rate, pressure ratio and efficiency) are analyzed, while much more information about the complex flow fields is ignored and wasted. Therefore, it might be significantly useful to mine more information from the flow fields which can be regarded as images and analyzed using deep learning algorithms.

## Funding Data

- National Major Science and Technology Project of China (Grant No. 2017-II-0004-0016; Funder ID: 10.13039/501100013076).
- Natural Science Foundation of China (Grant No. 51876097; Funder ID: 10.13039/501100001809).

## Nomenclature

$c$	= undetermined coefficient
$C$	= undetermined coefficient vector
$d$	= number of random space dimensions
$D$	= film hole diameter
$F$	= sensitivity of the response variable
$G$	= tip clearance
$\mathcal{G}$	= adjoint sensitivity
$H$	= heat loading at rotor tip
$H_0$	= heat loading at rotor tip of datum case
$L$	= film hole length
$M$	= leakage mass flow rate
$\mathcal{M}$	= correlation model
$M_0$	= leakage mass flow rate of datum case
$N$	= number of samples
$p$	= PC expansion order
$P$	= term number of PC expansion
$r$	= blade tip fillet radius
$\tilde{r}$	= Spearman rank correlation coefficient
$R$	= flow control equation
$Re_c$	= Reynolds number based on chord and inlet condition: $Re_c = \frac{\text{chord length} \times \text{kinematic viscosity}}{\text{freestream velocity}}$
$T$	= temperature
$T_{\text{crit}}$	= critical temperature
$T_{t1}$	= inlet total temperature
$T_{t2}$	= outlet total temperature
$X$	= uncertainty input variable
$Y$	= response variable
$\beta_1$	= inflow angle
$\beta_2$	= outflow angle
$\gamma$	= isentropic exponent
$\delta\varepsilon$	= geometric variable deformation
$\partial_i$	= relative weight of the $i$ -th sample
$\eta_{is}$	= isentropic efficiency: $\eta_{is} = \frac{\pi_t^{\gamma-1}-1}{T_{t2}/T_{t1}-1}$
$\zeta$	= independent random variables vector
$\nu$	= degree-of-freedom of Student's $t$ -distribution
$\pi_t$	= total-to-total pressure ratio
$\sigma$	= standard deviation

$\Phi$  = orthogonal polynomial  
 $\Psi$  = adjoint operator  
 $\omega$  = flow field variable

## Abbreviations

AM	= additive manufacturing
ANN	= artificial neural network
CFD	= computational fluid dynamics
EBPVD	= electron beam physical vapor deposition
HP	= high pressure
IPC	= intrusive polynomial chaos
LES	= large eddy simulation
LP	= low pressure
MC	= Monte Carlo
MCMLS	= Monte Carlo multilevel sampling
NIPC	= nonintrusive polynomial chaos
PC	= polynomial chaos
PCA	= principal component analysis
PDF	= probability density function
QMC	= quasi-Monte Carlo
RSM	= response surface model
SAMBA PC	= sparse approximation of moment-based arbitrary polynomial chaos
SVR	= support vector regression
UQ	= uncertainty quantification

## References

- [1] Schnell, R., Lengyel-Kampmann, T., and Nicke, E., 2014, "On the Impact of Geometric Variability on Fan Aerodynamic Performance, Unsteady Blade Row Interaction, and Its Mechanical Characteristics," *ASME J. Turbomach.*, **136**(9), p. 091005.
- [2] Garzon, V. E., 2003, "Probabilistic Aerothermal Design of Compressor Airfoils," *Ph.D. thesis*, Massachusetts Institute of Technology, Cambridge, MA.
- [3] Lamb, C. T., and Darmofal, D. L., 2004, "Performance-Based Geometric Tolerancing of Compressor Blades," *ASME Paper No. GT2004-53592*.
- [4] Montomoli, F., Carnevale, M., D'Ammaro, A., Massini, M., and Salvadori, S., 2019, *Uncertainty Quantification in Computational Fluid Dynamics and Aircraft Engines*, Springer, Cham, Switzerland.
- [5] Walters, R. W., and Huyse, L., 2002, "Uncertainty Analysis for Fluid Mechanics With Applications," NASA, Hampton, VA, Report No. *NASA CR-2002-211449*.
- [6] Maitre, O. L., and Knio, O. M., 2010, *Spectral Methods for Uncertainty Quantification: With Applications to Computational Fluid Dynamics*, Springer, Dordrecht, The Netherlands.
- [7] Najm, H. N., 2009, "Uncertainty Quantification and Polynomial Chaos Techniques in Computational Fluid Dynamics," *Annu. Rev. Fluid Mech.*, **41**(1), pp. 35–52.
- [8] Giebmanns, A., Backhaus, J., Frey, C., and Schnell, R., 2013, "Compressor Leading Edge Sensitivities and Analysis With an Adjoint Flow Solver," *ASME Paper No. GT2013-94427*.
- [9] Allaire, G., 2015, "A Review of Adjoint Methods for Sensitivity Analysis, Uncertainty Quantification and Optimization in Numerical Codes," *Ingénieurs de L'Automobile*, **83**(July 2015), pp. 33–36.
- [10] Walsh, P. P., and Fletcher, P., 2004, *Gas Turbine Performance*, Blackwell Science Ltd, Oxford, UK.
- [11] Mavromihales, M., Mason, J., and Weston, W., 2003, "A Case of Reverse Engineering for the Manufacture of Wide Chord Fan Blades (WCFB) Used in Rolls Royce Aero Engines," *J. Mater. Process. Technol.*, **134**(3), pp. 279–286.
- [12] Ramerth, D. L., MirzaMoghadam, A. V., Kirat Singh, A., and Banda, G., 2011, "A Probabilistic Secondary Flow System Design Process for Gas Turbine Engines," *ASME J. Eng. Gas Turbines Power*, **133**(9), p. 092502.
- [13] Zamboni, G., and Xu, L., 2012, "Fan Root Aerodynamics for Large Bypass Gas Turbine Engines: Influence on the Engine Performance and 3D Design," *ASME J. Turbomach.*, **134**(6), p. 061017.
- [14] Lange, A., Voigt, M., Vogeler, K., Schrapp, H., Johann, E., and Gummer, V., 2012, "Impact of Manufacturing Variability and Nonaxisymmetry on High-Pressure Compressor Stage Performance," *ASME J. Eng. Gas Turbines Power*, **134**(3), p. 032504.
- [15] Marson, E., 1992, "Effect of Manufacturing Deviations on Performance of Axial Flow Compressor Blading," *ASME Paper No. 92-GT-326*.
- [16] Elmstrom, M. E., Millsaps, K. T., Hobson, G. V., and Patterson, J. S., 2011, "Impact of Nonuniform Leading Edge Coatings on the Aerodynamic Performance of Compressor Airfoils," *ASME J. Turbomach.*, **133**(4), p. 041004.
- [17] Wheeler, A. P. S., Sofia, A., and Miller, R. J., 2009, "The Effect of Leading-Edge Geometry on Wake Interactions in Compressors," *ASME J. Turbomach.*, **131**(4), p. 041013.
- [18] Klapproth, J. F., 1950, "Approximate Relative-Total-Pressure Losses of an Infinite Cascade of Supersonic Blades With Finite Leading-Edge Thickness," NACA, Cleveland, OH, Report No. *NACA RM E9L21*.
- [19] Carter, A., and Applied Mechanics Group, 1961, "Blade Profiles for Axial-Flow Fans, Pumps, Compressors, etc.," *Proc. Inst. Mech. Eng.*, **175**(1), pp. 775–806.
- [20] Reid, L., and Urasek, D. C., 1973, "Experimental Evaluation of the Effects of a Blunt Leading Edge on the Performance of a Transonic Rotor," *ASME J. Eng. Gas Turbines Power*, **95**(3), pp. 199–204.
- [21] Goodhand, M. N., and Miller, R. J., 2011, "Compressor Leading Edge Spikes: A New Performance Criterion," *ASME J. Turbomach.*, **133**(2), p. 021006.
- [22] Herrig, L. J., Emery, J. C., and Erwin, J. R., 1951, "Effect of Section Thickness and Trailing-Edge Radius on the Performance of NACA 65-Series Compressor Blades in Cascade at Low Speeds," NACA, Hampton, VA, Report No. *NACA RM L5 LJ16*.
- [23] Jia, Z. W., Jiang, T., and Li, Y. H., 2002, "Measurement of Dynamic Clearance Between Compressor Blade Tip and Case," *Aviation Precis. Manuf. Technol.*, **38**(4), pp. 44–46.
- [24] Wang, X., Pan, H. W., Zhou, Y. Z., and Liu, Z. F., 2004, "Blade-Tip Clearance Analysis of a Gas Turbine Compressor," *J. Vib. Eng.*, **17**(s1), pp. 58–60.
- [25] Smith, L. H., 1970, "Casing Boundary Layers in Multistage Axial Compressors," *Flow Res. Blading*, A. L. S. Dzung, ed., Elsevier, Amsterdam, The Netherlands, pp. 275–304.
- [26] Sakulkaew, S., Tan, C. S., Donahoo, E., Cornelius, C., and Montgomery, M., 2013, "Compressor Efficiency Variation With Rotor Tip Gap From Vanishing to Large Clearance," *ASME J. Turbomach.*, **135**(3), p. 031030.
- [27] Zheng, X., and Yang, H., 2016, "Influence of Tip Clearance on the Performance and Matching of Multistage Axial Compressors," *ASME Paper No. GT2016-56232*.
- [28] Vo, H. D., 2001, "Role of Tip Clearance Flow on Axial Compressor Stability," *Ph.D. thesis*, Massachusetts Institute of Technology, Cambridge, MA.
- [29] Baghdadi, S., 1996, "Modeling Tip Clearance Effects in Multistage Axial Compressors," *ASME J. Turbomach.*, **118**(4), pp. 697–705.
- [30] Bons, J. P., 2010, "A Review of Surface Roughness Effects in Gas Turbines," *ASME J. Turbomach.*, **132**(2), p. 021004.
- [31] Moses, J. J., and Serovy, G. K., 1951, "Effect of Blade-Surface Finish on Performance of a Single-Stage Axial-Flow Compressor," NASA, Cleveland, OH, Report No. *NASA RME51c09*.
- [32] Gbadebo, S. A., Hynes, T. P., and Cumpsty, N. A., 2004, "Influence of Surface Roughness on Three-Dimensional Separation in Axial Compressors," *ASME J. Turbomach.*, **126**(4), pp. 455–463.
- [33] Debruge, L. L., 1980, "The Aerodynamic Significance of Fillet Geometry in Turbocompressor Blade Rows," *ASME J. Eng. Power*, **102**(4), pp. 984–993.
- [34] Hoeger, M., Schmidt-Eisenlohr, U., Gomez, S., Sauer, H., and Müller, R., 2002, "Numerical Simulation of the Influence of a Fillet and a Bulb on the Secondary Flow in a Compressor Cascade," *Task Q.*, **6**(1), pp. 25–37.
- [35] Goodhand, M. N., and Miller, R. J., 2012, "The Impact of Real Geometries on Three-Dimensional Separations in Compressors," *ASME J. Turbomach.*, **134**(2), p. 021007.
- [36] Wisler, D. C., 1985, "Loss Reduction in Axial-Flow Compressors Through Low-Speed Model Testing," *ASME J. Eng. Gas Turbines Power*, **107**(2), pp. 354–363.
- [37] Moeckel, C. W., Darmofal, D. L., Kingston, T. R., and Norton, R. J., 2007, "Toleranced Designs of Cooled Turbine Blades Through Probabilistic Thermal Analysis of Manufacturing Variability," *ASME Paper No. GT2007-28009*.
- [38] Montomoli, F., Massini, M., and Salvadori, S., 2011, "Geometrical Uncertainty in Turbomachinery: Tip Gap and Fillet Radius," *Comput. Fluids*, **46**(1), pp. 362–368.
- [39] Watt, R. M., Allen, J. L., Baines, N. C., Simons, J. P., and George, M., 1988, "A Study of the Effects of Thermal Barrier Coating Surface Roughness on the Boundary Layer Characteristics of Gas Turbine Aerofoils," *ASME J. Turbomach.*, **110**(1), pp. 88–93.
- [40] Jovanović, M. B., De Lange, H. C., and Van Steenhoven, A. A., 2008, "Effect of Hole Imperfection on Adiabatic Film Cooling Effectiveness," *Int. J. Heat Fluid Flow*, **29**(2), pp. 377–386.
- [41] Allmen, M., and Blatter, A., 1995, *Laser-Beam Interactions With Materials: Physical Principles and Applications*, Springer, Berlin.
- [42] Stimpson, C. K., Snyder, J. C., Thole, K. A., and Mongillo, D., 2018, "Effectiveness Measurements of Additively Manufactured Film Cooling Holes," *ASME J. Turbomach.*, **140**(1), p. 011009.
- [43] Stimpson, C. K., Snyder, J. C., Thole, K. A., and Mongillo, D., 2017, "Scaling Roughness Effects on Pressure Loss and Heat Transfer of Additively Manufactured Channels," *ASME J. Turbomach.*, **139**(2), p. 021003.
- [44] Bunker, R. S., 2009, "The Effects of Manufacturing Tolerances on Gas Turbine Cooling," *ASME J. Turbomach.*, **131**(4), pp. 81–96.
- [45] Bogard, D. G., and Thole, K. A., 2006, "Gas Turbine Film Cooling," *J. Propulsion Power*, **22**(2), pp. 249–270.
- [46] Meher-Homji, C. B., Chaker, M. A., and Motiwala, M., 2001, "Gas Turbine Performance Deterioration," *Proceedings of the 30th Turbomachinery Symposium*, Turbomachinery Laboratories, Texas A&M University, Houston, TX, Sept. 17–20, pp. 139–176.
- [47] Sallee, G. P., Kruckenberg, H. D., and Toomey, E. H., 1975, "Analysis of Turbopfan Engine Performance Deterioration and Proposed Follow-on Tests," NASA, Cleveland, OH, Report No. *NASA CR-134769*.
- [48] Ju, Y., and Zhang, C., 2016, "Robust Design Optimization Method for Centrifugal Impellers Under Surface Roughness Uncertainties Due to Blade Fouling," *Chin. J. Mech. Eng.*, **29**(2), pp. 301–314.
- [49] Qin, R., Ju, Y., Wang, Y., and Zhang, C., 2016, "Flow Analysis and Uncertainty Quantification of a 2D Compressor Cascade With Dirty Blades," *ASME Paper No. GT2016-56915*.

- [50] Hamed, A., Tabakoff, W. C., and Wenglarz, R. V., 2006, "Erosion and Deposition in Turbomachinery," *J. Propulsion Power*, **22**(2), pp. 350–360.
- [51] Ghenaiet, A., 2012, "Study of Sand Particle Trajectories and Erosion Into the First Compression Stage of a Turbofan," *ASME J. Turbomach.*, **134**(5), p. 051025.
- [52] Ghenaiet, A., Tan, S. C., and Elder, R. L., 2005, "Prediction of an Axial Turbomachine Performance Degradation Due to Sand Ingestion," *Proc. Inst. Mech. Eng., Part A: J. Power Energy*, **219**(4), pp. 273–287.
- [53] Roberts, W. B., 1984, "Axial Compressor Performance Restoration by Blade Profile Control," *ASME Paper No. 84-GT-232*.
- [54] Mirzamoghadam, A. V., 2008, "Gas Turbine Plant Thermal Performance Degradation Assessment," *ASME Paper No. GT2008-50032*.
- [55] Meher-Homji, C. B., Focke, A. B., and Wooldridge, M. B., 1989, "Fouling of Axial Flow Compressors—Causes, Effects, Detection, and Control," *Proceedings of the 18th Turbomachinery Symposium*, Turbomachinery Laboratories, Texas A&M University, Houston, TX, Sept. 18–21, pp. 55–76.
- [56] Bons, J. P., Taylor, R. P., McClain, S. T., and Rivir, R. B., 2001, "The Many Faces of Turbine Surface Roughness," *ASME J. Turbomach.*, **123**(4), pp. 739–748.
- [57] Kurz, R., and Brun, K., 2001, "Degradation in Gas Turbine Systems," *ASME J. Eng. Gas Turbines Power*, **123**(1), pp. 70–77.
- [58] Suder, K. L., Chima, R. V., Strazisar, A. J., and Roberts, W. B., 1995, "The Effect of Adding Roughness and Thickness to a Transonic Axial Compressor Rotor," *ASME J. Turbomach.*, **117**(4), pp. 491–505.
- [59] Mezheritsky, A. D., and Sudarev, A. V., 1990, "The Mechanism of Fouling and the Cleaning Technique in Application to Flow Parts of the Power Generation Plant Compressors," *ASME Paper No. 90-GT-103*.
- [60] Caguiat, D. E., 2003, "Rolls Royce/Allison 501-K Gas Turbine Antifouling Coatings Evaluation," *ASME J. Turbomach.*, **125**(3), pp. 482–488.
- [61] Bammert, K., and Sandstede, H., 1972, "Measurements Concerning the Influence of Surface Roughness and Profile Changes on the Performance of Gas Turbines," *ASME J. Eng. Power*, **94**(3), pp. 207–213.
- [62] Kellersmann, A., Weiler, S., Bode, C., Friedrichs, J., Städling, J., and Ramm, G., 2018, "Surface Roughness Impact on Low-Pressure Turbine Performance Due to Operational Deterioration," *ASME J. Eng. Gas Turbines Power*, **140**(6), p. 062601.
- [63] Tabakoff, W., Hamed, A., and Shanov, V., 1998, "Blade Deterioration in a Gas Turbine Engine," *Int. J. Rotating Mach.*, **4**(4), pp. 233–241.
- [64] Goward, G. W., 1986, "Low-Temperature Hot Corrosion in Gas Turbines: A Review of Causes and Coatings Therefor," *ASME J. Eng. Gas Turbines Power*, **108**(2), pp. 421–425.
- [65] Dundas, R. E., 1986, "A Study of the Effect of Deterioration on Compressor Surge Margin in Constant Speed, Single Shaft Gas Turbines," *ASME Paper No. 86-GT-177*.
- [66] Montomoli, F., and Massini, M., 2013, "Gas Turbines and Uncertainty Quantification: Impact of PDF Tails on UQ Predictions, the Black Swan," *ASME Paper No. GT2013-94306*.
- [67] Caflisch, R. E., 1998, "Monte Carlo and quasi-Monte Carlo Methods," *Acta Numer.*, **7**, pp. 1–49.
- [68] Kumar, A., 2006, "Robust Design Methodologies: Application to Compressor Blades," *Ph.D. thesis*, University of Southampton, Southampton, UK.
- [69] Eldred, M. S., Giunta, A. A., van Bloemen Waanders, B. G., Wojtkiewicz, S. F., Hart, W. E., and Alleva, M. P., 2006, "DAKOTA, a Multilevel Parallel Object-Oriented Framework for Design Optimization, Parameter Estimation, Uncertainty Quantification, and Sensitivity Analysis," Sandia National Laboratories, Albuquerque, NM, Report No. SAND2006-6337.
- [70] Wang, Q., 2009, "Uncertainty Quantification for Unsteady Fluid Flow Using Adjoint-Based Approaches," Stanford University, Stanford, CA.
- [71] Putko, M., Taylor Iii, A., Newman, P., and Green, L., 2001, "Approach for Uncertainty Propagation and Robust Design in CFD Using Sensitivity Derivatives," *AIAA Paper No. 2001-2528*.
- [72] Bose, D., Wright, M. J., and Palmer, G. E., 2006, "Uncertainty Analysis of Laminar Aeroheating Predictions for Mars Entries," *J. Thermophys. Heat Transfer*, **20**(4), pp. 652–662.
- [73] Myers, R. H., Montgomery, D. C., and Anderson-Cook, C. M., 2016, *Response Surface Methodology: Process and Product Optimization Using Designed Experiments*, Wiley, Hoboken, NJ.
- [74] He, X., and Zheng, X., 2017, "Performance Improvement of Transonic Centrifugal Compressors by Optimization of Complex Three-Dimensional Features," *Proc. Inst. Mech. Eng., Part G: J. Aerosp. Eng.*, **231**(14), pp. 2723–2738.
- [75] Constantine, P. G., Dow, E., and Wang, Q., 2014, "Active Subspace Methods in Theory and Practice: Applications to Kriging Surfaces," *SIAM J. Sci. Comput.*, **36**(4), pp. A1500–A1524.
- [76] Wiener, N., 1938, "The Homogeneous Chaos," *Am. J. Math.*, **60**(4), pp. 897–936.
- [77] Xiu, D., and Karniadakis, G. E., 2002, "The Wiener–Askey Polynomial Chaos for Stochastic Differential Equations," *SIAM J. Sci. Comput.*, **24**(2), pp. 619–644.
- [78] Ghanem, R. G., and Spanos, P. D., 2003, *Stochastic Finite Elements: A Spectral Approach*, Courier Corporation, Mineola, New York.
- [79] Ghanem, R., and Spanos, P. D., 1990, "Polynomial Chaos in Stochastic Finite Elements," *ASME J. Appl. Mech.*, **57**(1), pp. 197–202.
- [80] Debusschere, B. J., Najm, H. N., Pébay, P. P., Knio, O. M., Ghanem, R. G., and Le Maître, O. P., 2004, "Numerical Challenges in the Use of Polynomial Chaos Representations for Stochastic Processes," *SIAM J. Sci. Comput.*, **26**(2), pp. 698–719.
- [81] Parussini, L., and Pedriodra, V., 2007, "Fictitious Domain With Least-Squares Spectral Element Method to Explore Geometric Uncertainties by Non-Intrusive Polynomial Chaos Method," *Comput. Model. Eng. Sci.*, **22**(1), p. 416.
- [82] Loeven, G. J. A., and Bijl, H., 2008, "Probabilistic Collocation Used in a Two-Step Approach for Efficient Uncertainty Quantification in Computational Fluid Dynamics," *Comput. Model. Eng. Sci.*, **36**(3), pp. 193–212.
- [83] Ahlfeld, R., and Montomoli, F., 2017, "A Single Formulation for Uncertainty Propagation in Turbomachinery: SAMBA PC," *ASME J. Turbomach.*, **139**(11), p. 111007.
- [84] Rubinstein, R., and Choudhari, M., 2005, "Uncertainty Quantification for Systems With Random Initial Conditions Using Wiener–Hermite Expansions," *Stud. Appl. Math.*, **114**(2), pp. 167–188.
- [85] Drela, M., and Youngren, H. A., 1998, "User's Guide to MISES 2.53," Massachusetts Institute of Technology, Cambridge, MA.
- [86] Lange, A., Voigt, M., Vogeler, K., Schrapp, H., Johann, E., and Gummer, V., 2010, "Probabilistic CFD Simulation of a High-Pressure Compressor Stage Taking Manufacturing Variability Into Account," *ASME Paper No. GT2010-22484*.
- [87] Duffner, J. D., 2008, "The Effects of Manufacturing Variability on Turbine Vane Performance," *Aerospace Computational Design Laboratory*, Department of Aeronautics and Astronautics, Massachusetts Institute of Technology, Cambridge, MA.
- [88] Tang, X., Luo, J., and Liu, F., 2018, "Adjoint Aerodynamic Optimization of a Transonic Fan Rotor Blade With a Localized Two-Level Mesh Deformation Method," *Aerosp. Sci. Technol.*, **72**, pp. 267–277.
- [89] Wunsch, D., Hirsch, C., Nigro, R., and Coussement, G., 2015, "Quantification of Combined Operational and Geometrical Uncertainties in Turbo-Machinery Design," *ASME Paper No. GT2015-43399*.
- [90] D'Ammaro, A., and Montomoli, F., 2013, "Uncertainty Quantification and Film Cooling," *Comput. Fluids*, **71**, pp. 320–326.
- [91] Ghisu, T., Parks, G. T., Jarrett, J. P., and Clarkson, P. J., 2010, "Adaptive Polynomial Chaos for Gas Turbine Compression Systems Performance Analysis," *AIAA J.*, **48**(6), pp. 1156–1170.